International Journal of
INTELLIGENT SYSTEMS AND APPLICATIONS IN ENGINEERING
ISSN:2147-6799 www.ijisae.org Original Research Paper

Detection of Low Back Pain Based on Image Processing with Neural Network

[1]Mohammad Shahid, [2]Vetrimani, [3]Garima Sharma, [4]Ramesh Chandra Tripathi

Submitted: 15/04/2023 **Revised**: 17/06/2023 **Accepted**: 28/06/2023

Abstract*:* Low back pain is a common ailment affecting a significant portion of the global population. Accurate and timely detection of the causes and severity of low back pain is crucial for effective treatment and management. Traditional diagnosis methods for low back pain often rely on subjective assessments and are prone to inter-observer variability. In recent years, image processing techniques have emerged as valuable tools for analyzing medical images and providing objective diagnostic information. In this study, we propose a novel remora-optimized deep neural network (RODNN) approach for detecting low back pain. Initially, we gathered an MRI dataset of the lumbar region to evaluate the effectiveness of the proposed method. These images are pre-processed using a Gaussian filter for noise reduction. Followed by, grey level co-occurrence matrix (GLCM) is used to extract the relevant features. The experimental results are analyzed regarding the accuracy, precision, recall, and f1-score metrics. Practical outcomes demonstrate the superior performance of the proposed RO-DNN technique in low back pain detection when compared to existing approaches.

Keywords: *Low back pain, remora optimized deep neural network (RODNN), MRI image, lumbar region*

1. Introduction

A large percentage of people throughout the world experience low back pain (LBP), which is a prevalent medical problem. It is a major contributor to disability and frequently negatively affects productivity, quality of life, and healthcare expenses. For low back pain to be effectively treated and managed, the underlying reasons must be accurately and promptly identified. Magnetic resonance imaging (MRI) is a method that has attracted a lot of attention recently for the diagnosis of LBP. It is thought to impact 60–70% of people at some point in their lives and affects people of all ages [1]. The effects of LBP can range from minor aches to severe pain and functional impairment, which frequently impairs one's capacity to carry out everyday duties and jobs associated with work. The interior structures of the lumbar spine can be seen in great detail using non-invasive magnetic resonance imaging (MRI) [2]. Compared to other imaging modalities like X-ray or computed tomography (CT), it gives higher soft tissue contrast. A wide variety of diseases, such as disc herniation, spinal stenosis, degenerative disc disease, and spinal tumors, can be seen with lumbar MRI and may be the cause of low back discomfort [3]. The ability to pinpoint these particular causes aids in selecting the best course of action for treatments like surgery, physical therapy, or medication. Multiple axial, sagittal, and coronal images of the lumbar spine are generally taken during lumbar MRI imaging. The anatomical structures and pathological alterations in the area can be evaluated in detail using these images. These images are examined by radiologists and medical professionals for anomalies such as disc protrusions, bulges, or nerve root impingement, among other pertinent findings [4]. Advanced imaging procedures such as dynamic contrast-enhanced MRI (DCE-MRI) and diffusion-weighted imaging (DWI) can offer more functional details about the spine. Due to the intricacy and variety of the human spine, interpreting lumbar MRI images can be difficult.

Expertise and experience are needed to detect abnormal features and their discrimination from normal anatomical components [5]. Additionally, the appearance of unrelated incidental findings that might or might not be connected to the patient's low back discomfort can raise doubts about the diagnosis. These issues highlight the value of highly qualified radiologists and multidisciplinary teams that include neurologists, orthopedic surgeons, and radiologists for accurate diagnosis and thoughtful treatment planning [6]. The interpretation of lumbar MRI images has shown promise for automation in recent years thanks to artificial

[1]*Associate Professor, Department of Artificial Intelligence & Machine Learning (AIML), Noida Institute of Engineering and Technology, Greater Noida, Uttar Pradesh, India, Email id: mohammadshahid@niet.co.in*
[2]*Assistant Professor, Department of Computer Science and Engineering, Presidency University, Bangalore, India, Email Id: vetrimani.elangovan@presidencyuniversity.in*
[3]*Assistant Professor, Department of Computer Science & Engineering, Vivekananda Global University, Jaipur, India, Email Id: garima.sharma@vgu.ac.in*
[4]*Professor, College of Computing Science and Information Technology, Teerthanker Mahaveer University, Moradabad, Uttar Pradesh, India, Email id: rctripathig@gmail.com*

intelligence (AI) methods, notably deep learning algorithms. To uncover trends and pinpoint specific pathologies related to low back pain, these algorithms can be trained on big datasets. AI-based methods could help radiologists by automating the detection and measurement of abnormalities, speeding up interpretation, and increasing the precision of the diagnosis. However, additional investigation and validation are required to guarantee the validity and applicability of these AI models in clinical settings [7].

The purpose of this research is to give a general overview of how lumbar MRI scans are used to identify low back discomfort. Mechanical, inflammatory, and degenerative factors are only a few of the many potential causes of low back pain, which is a complex disorder.

The remainder of the paper is divided into subsequent parts. Part 3 contains the proposed method explained. Part 4 includes the results and analysis. While Part 5 discusses the conclusions.

2. Related Works

The purpose of the study [8] was to examine whether or not individuals with and without low back pain have different lumbar spine textural traits. A total of 14 chronic LBP patients and 14 healthy participants were compared for weight, age, and gender. The best classifier were chosen using the Random Forests Algorithm. The goal of study [9] was to see if textural research and machine learning might help identify more precise magnetic resonance picturing predictions of low back pain [9].

Study [10] investigated the creation of a "clinical decision support system (CDSS)" to assist LBP patients in making self-referrals to primary care. In order to do this, we looked into the potential of supervised machine learning. They evaluated the results of the three classification models, namely the decision tree, random forest, and boosted tree, to determine which model performed the best and whether it could already be used in actual practice. Article [11] proposed "deep convolutional neural networks (CNNs)" to identify, categorize, and grade IDD. For training in identifying and scoring IDD, the deep learning CNN technique was utilized. By evaluating the scoring of the data set utilizing a computerized model, the outcomes of the training using the CNN technique were confirmed. In study [12], the expectancy for lung tumors was investigated using classification methods such back-propagation neural networks and decision trees. In order to improve future assessments of the relationships between SDoH and low back pain results and disparities, researchers investigated natural language processing (NLP) and inference (NLI) approaches to extract SDoH data from the "clinical notes of patients with chronic low back pain" (cLBP). Study [13] developed a hybrid system incorporating matching patterns and a word bag designs, as well as 2 machine learning methods (based on convolutional neural network (CNN) and RoBERTa transformer). Study [14] proposed a novel approach to categorize a lifting dataset without human feature extraction using a 2D convolutional neural network (CNN). Study [15] suggested K-Nearest-Neighbor to categorize lower back pain particularly as either normal or abnormal based on Twelve Range of Motion (ROM) parameters. In order to preprocess the information, they employed substitute values that were missing and certain characteristic approaches. Machine learning techniques like KNN were then used to identify lower back pain.

3. Proposed Method

3.1. Dataset

We did not have a publicly available dataset for a herniated lumbar disc in the axial view. Therefore, we evaluated our method using information gathered from our MRI scans from the university's hospital in Sousse. We first discovered the studies on 50 cases before expanding the data set to 150 patients, including numerous axial resonance pictures. The subjects' ages range from 14 to 81, with at least one disc herniation and other abnormalities. The collection contains T1 and T2 weighted images; however, the T2 axial views magnetic resonance picturing is particularly relevant.

3.2. Gaussian filter

A technique known as the Gaussian filter is used to filter the picture during the categorization process. The Gaussian function's shape is used to determine which method to use, which is a straight filter with weighted values for each component. This technique was picked because it can filter pictures by refining them depending on the idea that this filter has a kernel's center. The usually dispersed noise is effectively removed by this filter. The value of each component in the resulting Gaussian smoothness filter can be estimated or determined through

$$g(w,z) = \frac{1}{c} f^{\frac{w^2+z^2}{2\sigma^2}} \quad (1)$$

Where c is the normalizing constant, and σ is the Gaussian Kernel's standard deviation

3.3. GLCM

A statistical technique for feature extraction in image processing and computer vision is called a gray-level co-occurrence matrix (GLCM). Based on the values of the gray levels of the pixels, it captures the spatial relationship between pairs of pixels in an image. To extract texture information from photos, GLCM is frequently employed.

- Applying the suitable grayscale conversion algorithm will enable you to convert your image to grayscale if it isn't already.
- Describe the GLCM's characteristics: Choose the direction and distance between any pixel pairs you want to include in the GLCM. Consider horizontal pixel pairs, for instance, and choose a distance of 1 pixel.
- Explain gray-level quantization: Select the appropriate amount of gray levels. Usually, the dynamic range of the image governs this. If the image has an 8-bit depth, for instance, you might select 256 gray levels.
- Make a blank GLCM matrix by starting one with dimensions equal to the number of gray levels. A pair of gray-level values are represented by each element of the matrix as their frequency of occurrence.
- Iterate through the image, determining the pair of pixels corresponding to each pixel depending on the selected angle and distance.
- Update the GLCM matrix by increasing the associated element for each pair of pixels based on their respective gray-level values.

To ensure that the GLCM matrix represents probabilities rather than frequencies, normalize it by dividing each member by the total number of entries.

3.4. Remora optimization algorithm (ROA)

This section introduces the remora optimization algorithm; like many MAs, the ROA uses remora's biological traits—specifically, their parasite behavior—to finish the optimizing procedure. Swordfish, whales, and other animals can all be attached to by Remora. Remora can readily get food with the host's assistance.

In order to accomplish the worldwide and local search, ROA modified a portion of the location upgrading techniques of WOA and SFO. To choose between the WOA approach and the SFO strategy, ROA employs an integer input H (0 or 1). Therefore, in some ways, when handling optimization issues, the ROA will benefit from using both optimization strategies.

3.4.1. A free trip

The ROA does the global search using the SFO technique, which depends on the elite approach utilized in the swordfish algorithm. The following is an expression for the positioning update formula:

$$U_j(s+1) = W_{best}(s) - \left(rand \times \left(\frac{W_{best}(s)+W_{rand}(s)}{2}\right) - W_{rand}(s)\right) \quad (2)$$

Where $U_j(s+1)$ is a potential location for the ith remora, the present top ranking is $W_{best}(s)$. A remora ranking at random is called $rand$. Iteration number t denotes the current iteration. Additionally, and is a chance value between 0 and 1.

Remora may also alter the host based on its experiences. A new applicant ranking can be created in this scenario by:

$$U_j'(s+1) = U_j(s+1) + randm \times (U_j(s+1) - W_j(s) \quad (3)$$

Where the candidate location for the ith remora is $\mathrm{U}_j'(\mathrm{s}+1)$, the ith remora's previous ranking is indicated by $\mathrm{W}_j(\mathrm{s})$. Additionally, a properly dispersed random number is generated using rand.

3.4.2. Eating mindfully

To feed, remora can also adhere to humpback whales. Because of this, remora will move as humpback whales do. In ROA, localized searching is carried out using the WOA approach. In particular, the WOA bubble-net assaulting strategy is deployed. The following are the altered positions changing formulas:

$$U_j(s+1) = C \times f^b \times \cos(2\pi b) + W_{best}(s) \quad (4)$$

$$C = |W_{best}(s) - W_j(s)| \quad (5)$$

$$b = rand \times (a-1) + 1 \quad (6)$$

$$a = -\left(1 + \frac{s}{S}\right) \quad (7)$$

Where D stands for the separation between the remora and the meal, it is evident from Eqs. (6) and (7) that an is a randomized number between 2 and 1. And from -1 to -2, b falls linearly.

Additionally, to further enhance the quality of the solutions, remora can create a tiny step by utilizing the WOA process of encircling prey, which is depicted as follows:

$$W_j(s+1) = U_j(s+1) + B \times C' \quad (8)$$

$$B = 2 \times A \times rand - A \quad (9)$$

$$A = 2 \times \left(1 - \frac{s}{S}\right) \quad (10)$$

$$C' = U_j(s+1) - D \times W_{best}(s) \quad (11)$$

Where $W_j(s+1)$, the ith remora's is a freshly created spot. C stands for the remora variable, which in ROA is set to 0.1.

3.5 DNN

The depth of deep learning networks, or the plenty of node levels via which information flows in a multiphase pattern identification procedure, is what sets them apart from more widely used single-hidden-layer neural networks. Deep is a very technical term that refers to multiple buried layers. Based on the output of the preceding layers, every single layer of node trains on a unique collection of features. More complex properties that nodes can identify are produced as neural networks develop. Since they combine information from the preceding layer, this structure is called a feature hierarchy that increases complexity and abstraction. It enables deep learning networks to process huge, highly dimensional data sets with billions of variables that flow via non-linear functions. Take the function f, where the data are supplied by Wi, $e(Wi)$, with Wi normally being high-dimensional and e (Wi) being either 0 or 1. The objective is to use the data provided to locate a function e * that, possibly, is close to f such that forecasts can be made accurately. We have a group of variables that we apply to deep learning, which is largely a set of parametric stats.

$$e(W;\theta) \tag{12}$$

W represents both the inputs and the factor, which is frequently high dimensional. Finding a such that $e(W;\theta)$ approaches f is the objective. The network is referred to here as θ. The network consists of d functions.

$$e^{(c)}(\cdot,\theta)\cdots e^{(1)}(\cdot,\theta), \tag{13}$$

This will primarily be high-dimensional. With the help of the picture, the network may be depicted in figure 1.

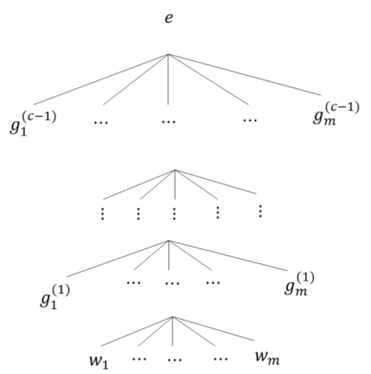

Fig.1. Network structure

Where $g_l^{(i)}$,..., $g_m^{(i)}$ are the elements of the vector-valued factor e^i, commonly known as the ith layer of the system, and each g_j^i is a function of $g_l^{(i-l)}$,..., $g_m^{(i-l)}$.

Although each f (i), which represents the width of surface i in the picture above, has an identical amount of elements, the width can generally vary from level to level. D stands for the network's depth. It's significant that the dth layer differs from the earlier layers in that its breadth is 1, or e = e^i is scalar-valued.

The model's result is provided by with the inputs denoted by w_1,..., w_m ∈ R.

$$e(W) = h\left(\sum b_j w_j + d\right) \tag{14}$$

It can be derived for certain non-linear functions g.

$$g^{(j)} = h^{\otimes}\,(X^{(j)^S} w + a^{(j)}) \tag{15}$$

Where g is a non-linear function that has been applied coordinate-wise.

The RELU function h(y) = max (0, y) is frequently used since, in general, g is the lowest non-linear function that is available. The logistic function is another option for g (driven by statistics and neurology).

$$h(y) = \frac{1}{1+f^{-2\beta y}}$$
(16)

As well as the hyperbolic tangent.

$$h(y) = tang(y) = \frac{f^y - f^{-y}}{f^y + f^{-y}}$$
(17)

4. Result

Performance analysis and model application are done on a computer with a Core i6 3.60 GHz CPU and 8 GB of RAM. This is carried out in Python. The effectiveness of the suggested strategy would be evaluated using the output metrics accuracy, recall, precisions, and F1-score. The significance of the proposed RO-DNN technique will be examined and contrasted with other methods such as Random Forest (RF), Decision Tree (DT), and CNN (Convolutional Neural Network).

The overall accuracy of the model's predictions is measured by accuracy. It is the proportion between the number of accurate and all other predictions combined. Accuracy offers a comprehensive evaluation of the model's performance. Regarding RO-DNN, the suggested strategy performs better (figure 2).

$$Accurcy = \frac{TPV+TNV}{TPV+TNV+FPV+FNV} \tag{18}$$

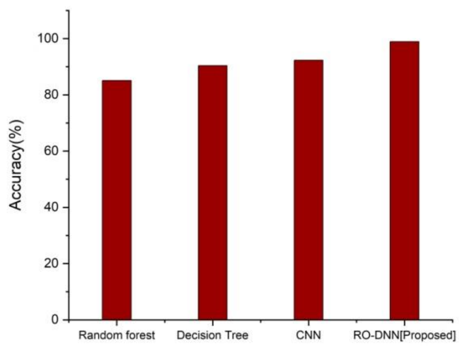

Fig.2. Accuracy

The model's accuracy in identifying positive events among those it predicted as positive is known as its "recision." It is the proportion of accurate predictions to the total of both accurate and inaccurate predictions that are positive. Precision is useful when false positives are expensive or undesired since it focuses on reducing false positives. Regarding RO-DNN, the suggested strategy performs better (figure 3).

$$Precision = \frac{TPV}{TPV+FPV} \tag{19}$$

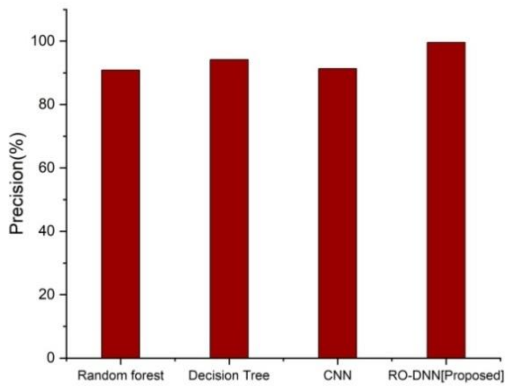

Fig.3. Precision

The model's capacity to distinguish accurately between positive instances from the real positive occurrences in the data is measured by a recall, also known as sensitivity or true positive rate. It is the proportion of accurate predictions to the total of both valid and inaccurate predictions. The recall is especially helpful when capturing as many positive instances as feasible are important or when false negatives are expensive. Regarding RO-DNN, the suggested strategy performs better (figure 4).

$$Recall = \frac{TPV}{TPV+FNV} \tag{20}$$

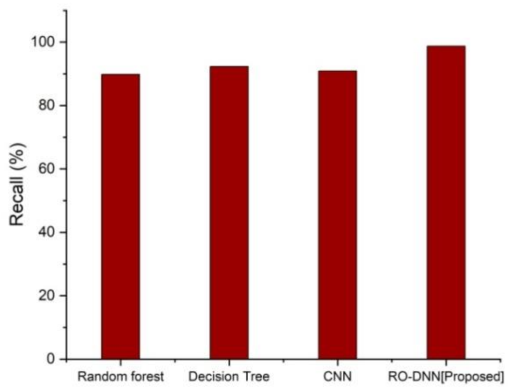

Fig.4. Recall

A harmonic mean of recall and precision is the F1-score. It offers a statistic that strikes a compromise between precision and recall. As 2 * ((precision * recall) / (precision + recall)), the F1-score is determined. It is a helpful indicator when the data's class distribution is uneven or when the importance of false positives and false negatives is equal. Regarding RO-DNN, the suggested strategy performs better (figure 5).

$$F1 - score = \frac{2TPV}{2TPV+FPV+FNV} \tag{21}$$

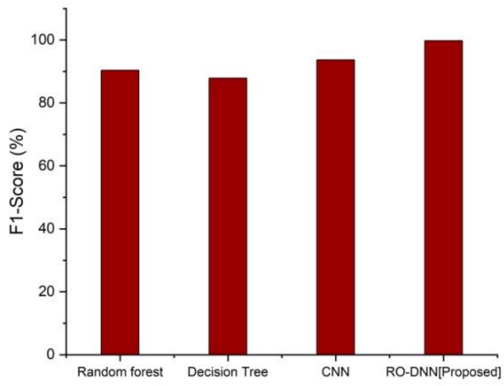

Fig.5. f1-score

5. Conclusion

The detection of low back pain using image processing and neural networks has the potential to significantly improve the diagnosis and management of this widespread condition. Neural networks can help detect important features and patterns in medical pictures related to low back pain by utilizing cutting-edge methods for image analysis and machine learning. In this study, a unique remora-optimized deep neural network (RODNN) method for the identification of low back discomfort is proposed. To assess the effectiveness of the suggested strategy, we first collect MRI data from the lumbar region. To reduce noise, these photos have undergone pre-processing using a Gaussian filter. The appropriate features are then extracted using the grey-level co-occurrence matrix (GLCM). Deep neural networks (DNNs) have drawbacks, including reliance on data, computing demands, interpretability, and susceptibility to hostile attacks. Future use of our suggested strategy for employing MRIs to analyze other diseases will be advantageous.

References

[1] Zheng, X., Reneman, M.F., Echeita, J.A., Preuper, R.H.S., Kruitbosch, H., Otten, E. and Lamoth, C.J., 2022. Association between central sensitization and gait in chronic low back pain: Insights from a machine learning approach. Computers in biology and medicine, 144, p.105329.

[2] Shafshak, T.S. and Elnemr, R., 2021. The visual

analog scale versus numerical rating scale in measuring pain severity and predicting disability in low back pain. JCR: Journal of Clinical Rheumatology, 27(7), pp.282-285.

[3] Ghai, B., Bansal, D., Kanukula, R., Gudala, K., Sachdeva, N., Dhatt, S.S. and Kumar, V., 2017. Vitamin D supplementation in patients with chronic low back pain: an open-label, single arm clinical trial. Pain physician, 20(1), p.E99.

[4] Apaydin, M., Uluc, M.E. and Sezgin, G., 2019. The lumbosacral transitional vertebra in the young men population with low back pain: anatomical considerations and degenerations (transitional vertebra types in the young men population with low back pain). La radiologia medica, 124, pp.375-381.

[5] Nicolson, P.J., Bennell, K.L., Dobson, F.L., Van Ginckel, A., Holden, M.A. and Hinman, R.S., 2017. Interventions to increase adherence to therapeutic exercise in older adults with low back pain and/or hip/knee osteoarthritis: a systematic review and meta-analysis. British Journal of sports medicine, 51(10), pp.791-799.

[6] Amorim, A.B., Pappas, E., Simic, M., Ferreira, M.L., Jennings, M., Tiedemann, A., Carvalho-e-Silva, A.P., Caputo, E., Kongsted, A. and Ferreira, P.H., 2019. Integrating Mobile-health, health coaching, and physical activity to reduce the burden of chronic low back pain trial (IMPACT): a pilot randomized controlled trial. BMC musculoskeletal disorders, 20, pp.1-14.

[7] Cherkin, D., Balderson, B., Wellman, R., Hsu, C., Sherman, K.J., Evers, S.C., Hawkes, R., Cook, A., Levine, M.D., Piekara, D. and Rock, P., 2018. Effect of low back pain risk-stratification strategy on patient outcomes and care processes: the MATCH randomized trial in primary care. Journal of general internal medicine, 33, pp.1324-1336.

[8] Abdollah, V., Parent, E.C., Dolatabadi, S., Marr, E., Croutze, R., Wachowicz, K. and Kawchuk, G., 2021. Texture analysis in the classification of T2-weighted magnetic resonance images in persons with and without low back pain. Journal of Orthopaedic Research®, 39(10), pp.2187-2196.

[9] Ketola, J.H., Inkinen, S.I., Karppinen, J., Niinimäki, J., Tervonen, O. and Nieminen, M.T., 2021. T2-weighted magnetic resonance imaging texture as predictor of low back pain: A texture analysis-based classification pipeline to symptomatic and asymptomatic cases. Journal of Orthopaedic Research®, 39(11), pp.2428-2438.

[10] Nijeweme-d'Hollosy, W.O., van Velsen, L., Poel, M., Groothuis-Oudshoorn, C.G., Soer, R. and Hermens, H., 2018. Evaluation of three machine learning models for self-referral decision support on low back pain in primary care. International journal of medical informatics, 110, pp.31-41.

[11] Liawrungrueang, W., Kim, P., Kotheeranurak, V., Jitpakdee, K. and Sarasombath, P., 2023. Automatic detection, classification, and grading of lumbar intervertebral disc degeneration using an artificial neural network model. Diagnostics, 13(4), p.663.

[12] Varadharajan, R., Priyan, M.K., Panchatcharam, P., Vivekanandan, S. and Gunasekaran, M., 2018. A new approach for prediction of lung carcinoma using back propogation neural network with decision tree classifiers. Journal of Ambient Intelligence and Humanized Computing, pp.1-12.

[13] Lituiev, D., Lacar, B., Pak, S., Abramowitsch, P.L., De Marchis, E. and Peterson, T., 2022. Automatic extraction of social determinants of health from medical notes of chronic lower back pain patients. medRxiv, pp.2022-03.

[14] Snyder, K., Thomas, B., Lu, M.L., Jha, R., Barim, M.S., Hayden, M. and Werren, D., 2021. A deep learning approach for lower back-pain risk prediction during manual lifting. Plos one, 16(2), p.e0247162.

[15] Sandag, G.A., Tedry, N.E. and Lolong, S., 2018, August. Classification of lower back pain using K-Nearest Neighbor algorithm. In 2018 6th International Conference on Cyber and IT Service Management (CITSM) (pp. 1-5). IEEE.

[16] Mr. Vaishali Sarangpure. (2014). CUP and DISC OPTIC Segmentation Using Optimized Superpixel Classification for Glaucoma Screening. International Journal of New Practices in Management and Engineering, 3(03), 07 - 11. Retrieved from http://ijnpme.org/index.php/IJNPME/article/view/30

[17] Reddy V, S. ., Madhav, V. ., M, B. ., Krishna A, A. ., A, K. ., Inthiyaz, S. ., & Ahammad, S. H. . (2023). Hybrid Autonomous Vehicle (Aerial and Grounded). International Journal on Recent and Innovation Trends in Computing and Communication, 11(1), 103–109. https://doi.org/10.17762/ijritcc.v11i1.6056